

On peculiarities of the annealing process for highly transparent silica based aerogel tiles manufactured in Novosibirsk

A.Yu. Barnyakov^{a,b}, A.F. Danilyuk^c, A.A. Kattsin^{a,d,*}, E.A. Kravchenko^{a,d}

^a*Budker Institute of Nuclear Physics, Acad. Lavrentiev Prospect 11, Novosibirsk, 630090, Russia*

^b*Novosibirsk State Technical University, Karl Marks Prospect 20, Novosibirsk, 630073, Russia*

^c*Borekov Institute of Catalysis, Acad. Lavrentiev Prospect 5, Novosibirsk, 630090, Russia*

^d*Novosibirsk State University, St. Pirogova 1, Novosibirsk, 630090, Russia*

Abstract

A collaboration between the Borekov Institute of Catalysis and the Budker Institute of Nuclear Physics (BINP) has been producing silica aerogel blocks for Cherenkov detectors since 1986. Novosibirsk-manufactured aerogel is used in several experiments: KEDR and SND (BINP, Russia), LHCb (CERN, Switzerland), AMS-02 (ISS), and CLAS12 RICH (Jefferson Lab, USA).

This work describes key advancements in the production technology for large-scale aerogel radiators used in Ring-Imaging Cherenkov (RICH) detectors. Annealing is one of the major stages of the highly transparent aerogel production in Novosibirsk. Its procedure was investigated in detail and optimized to improve the yield of aerogel tiles useful for the RICH detectors. The optical and mechanical parameters of the largest silica aerogel samples produced in Novosibirsk using the new annealing procedure are presented.

Keywords: Aerogel, Cherenkov detectors, RICH

1. Introduction

The production of the aerogel for Cherenkov counters began in Novosibirsk in 1986. Novosibirsk aerogel was used in the construction of the threshold Cherenkov counters for the KEDR experiment (aerogel $n = 1.05$, total volume ~ 1000 L) [1], for the experiment SND (aerogel $n = 1.13$, total volume ~ 9 L) [2], and DiRAC-II experiments (aerogel $n = 1.008$, total volume ~ 9 L) [3].

Since 2004, Novosibirsk aerogel has found application in several RICH (Ring-Imaging Cherenkov) detectors, including the RICH2 detector of the LHCb experiment (aerogel $n = 1.03$, area ~ 0.5 m², tile size $20 \times 20 \times 5$ cm³) [4], the RICH counter for the AMS-02 experiment (aerogel $n = 1.05$, area ~ 1 m², tile size 12.5×12.5 cm²) [5], and the RICH detector of the CLAS12 experiment (aerogel $n = 1.05$, area ~ 6 m², tile size $20 \times 20 \times 3$ – (2) cm³) [6].

For the RICH detectors, in addition to optical properties, the geometrical parameters of the radiators are critically important: flatness, thickness tolerance, and dimensions. Imperfections at the radiator edges can lead either to a loss of Cherenkov photons or to distortions in their spatial distribution, consequently degrading the particle identification performance. Therefore, in such detectors, it is desirable to minimize the total length of boundaries between individual radiators and to maximize the area of monolithic elements; consequently, it is important to produce aerogel tiles with the largest possible transverse size.

The production cycle of the high-transparency Novosibirsk aerogel can be conditionally divided into three main stages:

- **The Chemical synthesis** – where the key target parameters of the material are defined.
- **The Supercritical drying** – the stage where the aerogel itself is formed.

*Corresponding author

Email address: A.A.Kattsin@inp.nsk.su (A.A. Kattsin)

- **The Primary annealing** – a process during which the maximum transparency of the aerogel is achieved by removing residual organic solvents from its internal pores.

In 2022–2023, a detailed study of the primary annealing process was carried out. This allowed us to optimize the procedure and to significantly increase the useful yield of the large aerogel samples suitable for use in the RICH detectors. As a result, the first production of the monolithic blocks measuring $230 \times 230 \times 40 \text{ mm}^3$ with a refractive index of $n = 1.05$, as well as four-layer focusing blocks with a maximum refractive index of $n_{\text{max}} = 1.05$ and dimensions of $230 \times 230 \times 35 \text{ mm}^3$, were achieved in 2023.

2. Analysis of aerogel during thermal processing

Large silica aerogel tiles occasionally fracture during the primary annealing stage, which is designed to remove alcohol groups chemically bounded to the aerogel surface, organic impurities and residual chemicals after supercritical drying. To investigate this issue, thermogravimetric and differential scanning calorimetry analysis was conducted. The ThermoGravimetric Analysis (TGA) measures the mass change of the sample during controlled heating, while the Differential Scanning Calorimetry (DSC) monitors heat flow to detect endothermic (heat absorption) or exothermic (heat release) processes, such as organic decomposition or phase transitions.

Ground silica aerogel samples (10.82 mg) were heated from $22 \text{ }^\circ\text{C}$ to $450 \text{ }^\circ\text{C}$ at $5 \text{ }^\circ\text{C}/\text{min}$ in air. The mass loss (TG), its derivative (DTG), and the heat flow (DSC) were recorded (see Fig. 1).

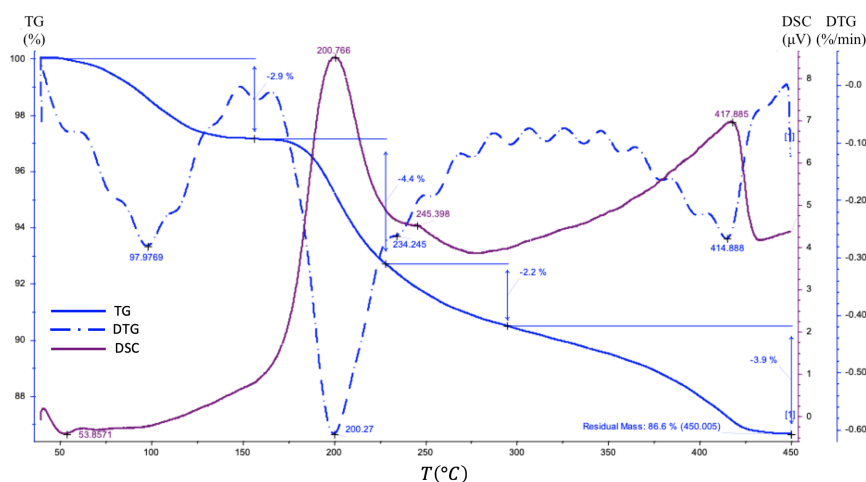


Figure 1: TG (blue), DTG (blue dash-dotted) and DSC (maroon) curves of silica aerogel combustion.

Three distinct stages are observed:

- Stage 1 (up to $100 \text{ }^\circ\text{C}$): endothermic desorption of water and volatiles;
- Stage 2 ($170\text{--}200 \text{ }^\circ\text{C}$): exothermic combustion of organics, rapid mass loss;
- Stage 3 ($417 \text{ }^\circ\text{C}$): secondary exothermic peak, likely oxidation of residual carbon.

Based on these results, the annealing procedure was modified to reduce cracking (see Section 3). The main assumption is that cracks occur at the points where heat is released very rapidly.

3. Optimization of the primary annealing protocol

The revised annealing protocol consists of slow, controlled heating steps:

- 1) Heat to $100 \text{ }^\circ\text{C}$ at $4 \text{ }^\circ\text{C}/\text{h}$ (20 h),

- 2) Then to 120 °C at 3 °C/h (6.5 h),
- 3) Then to 160 °C at 1.5 °C/h (26.5 h),
- 4) Hold at 160 °C for 500 min (organic burnout),
- 5) Heat to 470 °C at 5 °C/h (62 h),
- 6) Hold at 470 °C for 200 min (final combustion),
- 7) Cool to 50 °C at 10 °C/h (42 h).

Previously, the heating rate was 5 °C/h directly to 470 °C, followed by the 2 h hold and cooling at 10 °C/h. The new protocol enables slow organic removal while preserving aerogel integrity.

Using this method, we fabricated four-layer focusing aerogel tiles ($230 \times 230 \times 35 \text{ mm}^3$) for the first time. Some characteristics are given in Section 4. We also produced large-format aerogel blocks with refractive index of 1.05 and thickness of 40 mm (see Section 5).

4. The largest multilayer aerogel radiator

In multilayer aerogels, layer refractive indices and thicknesses are chosen so that Cherenkov rings from all layers coincide at the photon detector plane. Novosibirsk group has pioneered the production of monolithic multilayer aerogels with controlled refractive indices [7]. The first multilayer monolithic aerogel block produced in 2004 is shown in Fig. 2 (left). Building on this legacy, our 2023 advancements include the successful fabrication of multiple four-layer focusing aerogel samples ($230 \times 230 \times 35 \text{ mm}^3$), which meet targeted specifications for the refractive index and transparency (see Fig. 2 (right)).

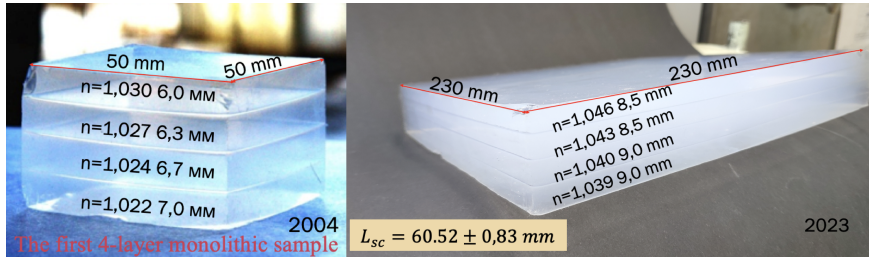


Figure 2: The first four-layer sample produced in 2004 (left). The four-layer tile produced in 2023 (right).

The refractive index of Novosibirsk-produced aerogels is related to density by empirical law [8]

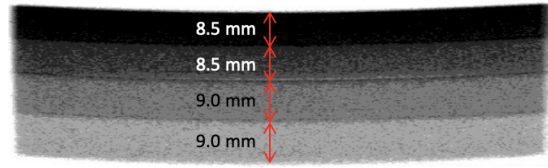
$$n = \sqrt{1 + 0.438\rho}, \quad (1)$$

where n is the refractive index of the aerogel, ρ is the aerogel density in g/cm^3 .

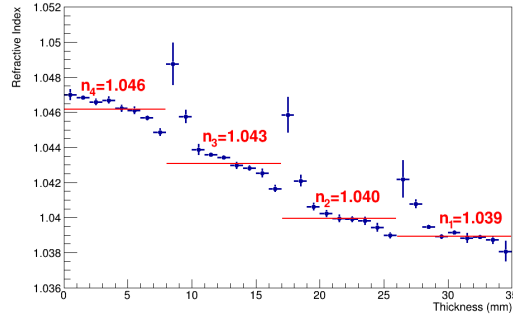
Layer indices are measured by an X-ray method [9]. The thickness distribution profile of the refractive index measured using the X-ray setup is shown in Fig. 3. Several large four-layer aerogel tiles were produced. The variations in their parameters make it possible to evaluate the precision and tolerances of the multilayer aerogel manufacturing technology. The refractive index (n_i) values for the specific layers of the four-layer aerogels 461f10 and 461f5 are given in Table 1.

Given the significantly shorter Rayleigh scattering length compared to the absorption length in aerogels, this optical parameter can be derived from luminous transmittance measurements. The procedure of light scattering length measurement was described earlier [10]. Examples of the measured light scattering length for the four-layer aerogels 461f10 and 461f5 at a single point are shown in Fig. 4. Table 1 lists light scattering lengths L_{sc} at $\lambda = 400 \text{ nm}$.

In aerogel RICH detectors, the Cherenkov angle resolution is affected by the surface planarity (Δ) of the tiles, which is defined as the peak-to-valley surface variation normalized to the lateral dimension [11].



(a) X-ray image of aerogel tile; darker areas indicate higher density.



(b) Profile of aerogel tile.

Figure 3: X-ray image and profile of the 461f10 aerogel tile (side view).

The planarity of the aerogel tiles was measured using a mechanical setup. The tile was placed on a measurement stand, and the height was recorded at multiple points across its surface according to a predefined grid. An alignment procedure was applied to correct for the global tilt of the tile by fitting and subtracting linear components along two orthogonal directions. After this correction, the planarity was defined as the difference between the maximum and minimum measured heights [12].

Novosibirsk-manufactured 30 mm-thick aerogels exhibit exceptional surface planarity ($\Delta \leq 1\%$ of the lateral dimensions; for example, in the case of the tile measuring $200 \times 200 \text{ mm}^2$, the permissible planarity is $\leq 2 \text{ mm}$), meeting stringent detector specifications [11, 12]. Table 1 also presents the measured planarity values and the main aerogel parameters evaluated for the production batch of tiles using measurements of two samples, 461f5 and 461f10. This shows that the parameter variations within the small batch do not exceed the measurement uncertainties of the single sample.

Table 1

Parameters of four-layer monolithic aerogel (2023).

aerogel	layer thickness d_i, mm	refractive index of the layer n_i	light scattering length L_{sc}, mm	planarity Δ, mm
461f5	9.0	1.045 ± 0.001	62.31 ± 0.26	1.32
	9.0	1.043 ± 0.002		
	8.5	1.040 ± 0.002		
	7.9	1.038 ± 0.001		
461f10	8.5	1.046 ± 0.001	62.53 ± 0.31	1.40
	8.5	1.043 ± 0.002		
	9.0	1.040 ± 0.002		
	9.0	1.039 ± 0.001		
aerogel	8.75	1.046 ± 0.001	62.40 ± 0.20	1.36
	8.75	1.043 ± 0.001		
	8.75	1.040 ± 0.001		
	8.45	1.039 ± 0.001		

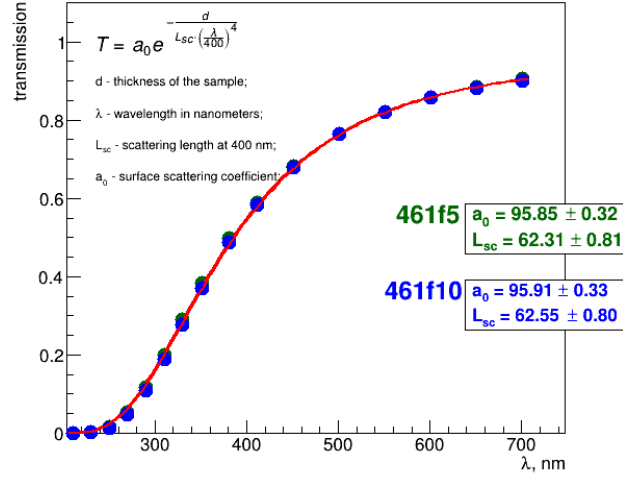


Figure 4: The transmittance of the focusing aerogel tiles 461f5 (blue markers) and 461f10 (green markers). The thickness is 35 mm.

These aerogel blocks were tested in details with the help of relativistic electrons at the BINP beam test facilities [13]. The single-photon resolution in the Cherenkov angle is about 7 mrad for a $3 \times 3 \text{ mm}^2$ pixel. In this experiment the pixel size varied using a shading mask as described in [14]. After subtracting the pixel contribution in quadrature, the intrinsic resolution of the focusing aerogel tile is estimated to be 5.6 mrad. This value is mainly determined by layer thickness (8–9 mm, contributing 4 mrad) and refractive index dispersion (4 mrad evaluated from GEANT4 simulations). The tests are presented in more detail in the article [15].

5. Thick aerogel radiator

Previously, the largest aerogel tiles from Novosibirsk were:

- $200 \times 200 \times 30 \text{ mm}^3$ for aerogel with refractive index of 1.05 [12];
- $200 \times 200 \times 50 \text{ mm}^3$ for aerogel with refractive index of 1.03 [4].

Changes of the primary annealing procedure allowed as the production of aerogels with $n = 1.05$ of unprecedented thickness. Fig. 5 (right) shows aerogel with the refractive index of 1.05 and the thickness of 40 mm — the record for this refractive index. Aerogel with the refractive index of 1.03 and the thickness of 50 mm was also reproduced, as shown in Fig. 5 (left). Table 2 summarises the parameters of aerogel tiles ($200 \times 200 \text{ mm}^2$). Examples of the measured light scattering length for the thick aerogels 461f13 and 460f9 at a single point are shown in Fig. 6.

Table 2
Parameters of thick aerogel tiles (2022–2023).

aerogel	thickness $d, \text{ mm}$	refractive index n	light scattering length $L_{sc}, \text{ mm}$	planarity $\Delta, \text{ mm}$
461f4	40	1.046	44.51 ± 0.19	1.99
460f9	40	1.050	44.75 ± 0.32	–
460f11	40	1.027	46.99 ± 0.35	1.90
461f14	40	1.028	50.09 ± 0.34	–
460f15	50	1.027	43.58 ± 0.33	–
461f13	50	1.028	50.00 ± 0.31	1.02

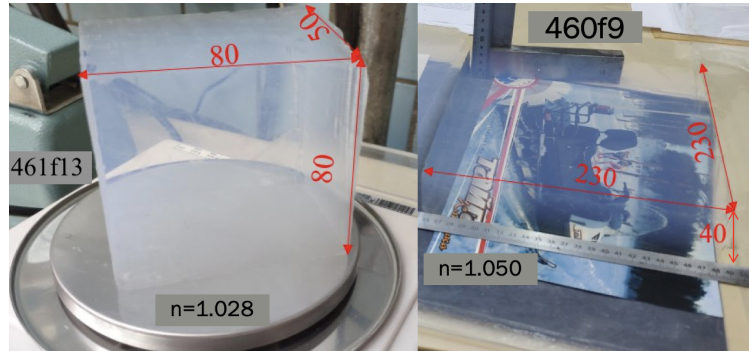


Figure 5: Thick aerogel tiles: sample 461f13, a quarter-tile ($n = 1.028$, thickness 50 mm), on the left and 460f9 ($n = 1.050$, thickness 40 mm) on the right.

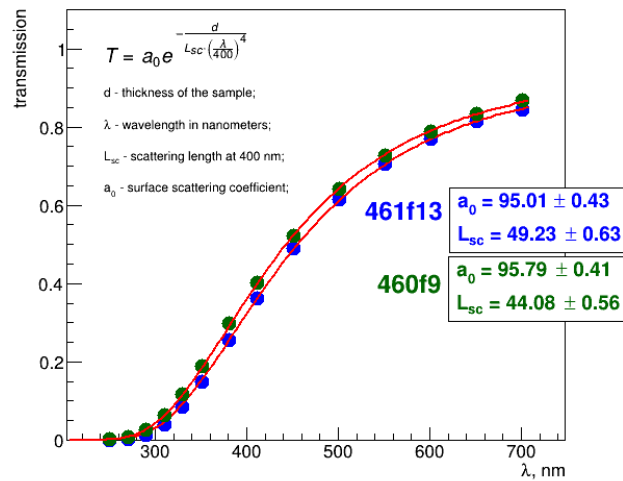


Figure 6: Transmittance of thick aerogel tiles: 461f13 ($n = 1.028$, thickness 50 mm, blue markers) and 460f9 ($n = 1.050$, thickness 40 mm, green markers).

6. Conclusion

In 2022–2023, significant progress was achieved in production of the aerogel-based Cherenkov radiators for the RICH detectors. Based on TGA/DSC analysis, the primary annealing procedure was optimized, to minimize crack formation in large tiles. Monolithic four-layer focusing tiles ($230 \times 230 \times 35 \text{ mm}^3$) with design refractive indices and high transparency were produced for the first time. The main aerogel parameters were evaluated for the production batch based on measurements of two samples, 461f5 and 461f10. The measured refractive indices of the layers are $n_1 = 1.039 \pm 0.001$, $n_2 = 1.040 \pm 0.001$, $n_3 = 1.043 \pm 0.001$, and $n_4 = 1.046 \pm 0.001$, while the light scattering length is $62.40 \pm 0.20 \text{ mm}$. The results show that the variation of these parameters within a small batch does not exceed the measurement uncertainties of a single sample. In addition, large, highly transparent blocks of aerogel with the refractive index of 1.05 and the thickness of 40 mm were produced — another world-first achievement.

Funding

The works were supported in part by the project Mirror Laboratories of HSE University.

Declaration of competing interest

The authors declare that they have no known competing financial interests or personal relationships that could have appeared to influence the work reported in this paper.

References

- [1] A. Yu. Barnyakov, et al., ASHIPH counters for the KEDR detector, *Nucl. Instr. and Meth. A* 494 (2002) 424–429. doi:10.1016/S0168-9002(02)01513-9.
- [2] A. Yu. Barnyakov, et al., High density aerogel for ASHIPH SND—test results, *Nucl. Instr. and Meth. A* 598 (2009) 163–165. doi:10.1016/j.nima.2008.08.018.
- [3] Y. Allkofer, et al., A new aerogel Cherenkov detector for DIRAC-II, *Nucl. Instr. and Meth. A* 595 (2008) 84–87. doi:10.1016/j.nima.2008.07.046.
- [4] T. Bellunato, The RICH detector of the LHCb experiment, *Nucl. Instr. and Meth. A* 598 (2009) 147–151. doi:10.1016/j.nima.2008.08.117.
- [5] M. Buenerd, The AMS02 Cherenkov imager prototype: In-beam tests with high-energy ions, *Nucl. Instr. and Meth. A* 553 (2005) 264–267. doi:10.1016/j.nima.2005.08.086.
- [6] M. Contalbrigo, et al., The CLAS12 large area RICH detector, *Nucl. Instr. and Meth. A* 639 (2011) 302–306. doi:10.1016/j.nima.2010.10.047.
- [7] A. Yu. Barnyakov, et al., Focusing aerogel RICH (FARICH), *Nucl. Instr. and Meth. A* 553 (2005) 70–75. doi:10.1016/j.nima.2005.08.073.
- [8] A. F. Danilyuk, et al., Recent results on aerogel development for use in Cherenkov counters, *Nucl. Instr. and Meth. A* 494 (2002) 491–494. doi:10.1016/S0168-9002(02)01537-1.
- [9] A. Yu. Barnyakov, et al., Cherenkov Detector with a Focusing Aerogel Radiator, in: eConf C0604032, 2006, p. 0045.
URL <http://www.slac.stanford.edu/econf/C0604032/papers/0045.PDF>
- [10] A. R. Buzykaev, et al., Measurement of optical parameters of aerogel, *Nucl. Instr. and Meth. A* 433 (1999) 396–400. doi:10.1016/S0168-9002(99)00325-3.
- [11] M. Contalbrigo, et al., Aerogel mass production for the CLAS12 RICH: Novel characterization methods and optical performance, *Nucl. Instr. and Meth. A* 876 (2017) 264–267. doi:10.1016/j.nima.2017.02.068.
- [12] A. Yu. Barnyakov, et al., The production of the large scale aerogel radiators for use in the Ring-imaging Cherenkov detectors, *Nucl. Instr. and Meth. A* 952 (2020) 162035. doi:10.1016/j.nima.2019.03.090.
- [13] G. N. Abramov, et al., Measurement of the energy of electrons extracted from the VEPP-4M accelerator, *JINST* 11 (2016) P03004. doi:10.1088/1748-0221/11/03/P03004.
- [14] A. Yu. Barnyakov, et al., PID system based on focusing aerogel RICH for the super C- τ factory, *Nucl. Instr. and Meth. A* 952 (2020) 162247. doi:10.1016/j.nima.2019.05.088.
- [15] A. Yu. Barnyakov, et al., R&D status of FARICH option for PID, *International Journal of Modern Physics A* 39 (26n27) (2024) 2442012. doi:10.1142/S0217751X24420120.